Nuclear Physics **A470** (1987) 609–625
North-Holland, Amsterdam

Σ^- HYPERNUCLEAR SPECTRA FROM (K^-, π^+) INCLUSIVE REACTIONS*

M. KOHNO[1], R. HAUSMANN[2], P. SIEGEL and W. WEISE

Institute of Theoretical Physics, University of Regensburg, D-8400 Regensburg, W. Germany

Received 18 March 1987

Abstract: We report on DWIA calculations of the pion inclusive spectra related to Σ-formation in (K^-, π^+) reactions on nuclei. Realistic distorted waves are used to describe the incoming kaon and outgoing pion. The Σ wave function is calculated in a real Woods-Saxon potential, the depth of which provides information about the underlying ΣN effective interaction. The absorptive effect due to the Σ-Λ conversion process in the nuclear medium is taken into account by effective two-channel coupled equations. Comparisons are made with the available data on ^{12}C and ^{16}O. Using a weak Σ-nucleus potential the overall agreement is satisfactory for the spectrum derived from kaon-in-flight experiments. Concerning the three peaks reported in a stopped kaon experiment on ^{12}C, the lowest peak structure can be generated by increasing the depth of the Σ potential in ^{12}C. However, the remaining two narrow structures cannot be reproduced as Σ-particle–proton–hole states in our continuum treatment of the Σ spectrum. The difficulties in extracting the strength of the Σ-nucleus spin-orbit potential are also discussed.

1. Introduction

Ever since the discovery of Σ hypernuclear states in (K^-, π) inclusive reactions [1]), the narrowness of Σ-formation peaks has been an intereresting and challenging problem. In kaon-in-flight experiments [1-3]) on ^{6}Li, ^{9}Be, ^{12}C and ^{16}O, peak structures with widths of about 5 MeV have been observed at excitation energies $\varepsilon_\Sigma =$ 2–10 MeV, which correspond to Σ-substitutional states reached with small momentum transfers. In a stopped kaon experiment [4]) on ^{12}C with a momentum transfer of about 170 MeV/c, three peaks have been reported with widths as small as 3 MeV. The puzzling question is why the Σ states acquire such a narrow width, in spite of their expected short lifetime in the nuclear medium due to the strong $\Sigma N \to \Lambda N$ conversion process, and in view of the fact that these states are unbound.

A number of authors [5,6]) have suggested that medium corrections such as Pauli blocking effects are able to reduce the Σ-conversion width substantially from its value estimated in nuclear matter ($\Gamma_\Sigma = 30 \pm 5$ MeV). In fact, reaction matrix calculations [7]) with the Nijmegen potential [8]) lead to $\Gamma_\Sigma \simeq 10$ MeV in nuclear matter. Gal *et al.* [9]) proposed a possible explanation of the narrowness of the Σ-formation peak in terms of an unstable bound state. However, the physical significance of the concept of unstable bound states in this context is not generally agreed on [10,11]).

* Work supported in part by BMFT, grant MEP 0234 REA.

[1] Present address: Division de Physique Théorique, Institut de Physique Nucléaire, F-91406 Orsay, Cedex, France.

[2] Supported by Studienstiftung des Deutschen Volkes.

A realistic discussion of the Σ-formation peaks requires an explicit calculation of the response function in this channel. In the DWIA (distorted wave impulse approximation) framework commonly used, the effect of the Σ-Λ conversion process is described by an imaginary optical potential $iW_\Sigma(r)$, the strength of which is related to Γ_Σ by $W_\Sigma^{(0)} = -\frac{1}{2}\Gamma_\Sigma$ (see eq. (15a)). Morimatsu and Yazaki [10]) presented a schematic treatment of the pion inclusive spectra using Green's function methods with a complex optical potential for the Σ in one calculation and a coupled channel scheme in a second one. Their calculations indicate that for a sufficiently small imaginary Σ-potential (or for a small Σ-Λ transition potential), a narrow peak can be obtained at low energy.

Another important issue in the investigation of Σ hypernuclei is the strength of the spin-orbit field experienced by the Σ in a nucleus, which is related to the strength of the two-body ΣN spin-orbit force. In view of a variety of theoretical studies based on quark models [12]) as well as meson exchange approaches [13]), it is hoped that the extraction of the ΣN spin-orbit strength from the experiments provides information on the underlying mechanisms of the ΣN interaction.

In this paper, we present detailed DWIA calculations of the (K^-, π^+) inclusive spectra associated with Σ-formation in nuclei, taking properly into account the Σ continuum states. We use realistic distorted wave functions for the incoming kaon and the outgoing pion. Almost all of the Σ states in question are unbound. We do not introduce a phenomenological imaginary Σ potential, but generate the wave functions explicitly by solving a simplified Σ-Λ coupled channels problem in each partial wave.

Our results for ^{12}C and ^{16}O show a good general correspondence with the experimental spectra observed in the kaon-in-flight experiment, although the detailed peak structure differs from one of the data sets in ref. [2]). In particular, our calculations suggest a weak Σ-nucleus average single-particle potential. With such a potential, no narrow peak structure is found in the spectrum corresponding to the stopped kaon experiment, in contrast to the three peaks reported in ref. [4]). What one can hope to achieve at best for the stopped kaon case is to reproduce one peak at an energy close to threshold by adjusting the Σ single-particle potential such that it is sufficiently weak not to generate a p-wave found state, but still strong enough to concentrate the p-wave strength in a narrow region at low energy. This phenomenological information on the Σ-nucleus potential sets a useful constraint in the study of the ΣN effective interaction in nuclei.

Apart from the work of Morimatsu and Yazaki already mentioned, several other calculations have recently become available which describe Σ hypernuclei with inclusion of a quasifree background. Kishimoto [14]) and Chrien *et al.* [15]) have used a pole graph method in the attempt to reproduce Σ-hypernuclear spectra entirely in terms of the quasifree continuum. Recently Zofka *et al.* [16]) have performed calculations in a continuum shell model.

Our treatment is somewhat similar to the coupled-channels approach of Morimatsu *et al.*, although we use a different formalism to construct the response function. We do not differentiate between "quasifree" and "resonant" parts of the Σ hypernuclear spectra, as is sometimes done, since both features should emerge naturally in a consistent coupled channels scheme.

We shall proceed as follows. In sect. 2, we summarize our calculational scheme of the DWIA response function. The distorted wave functions for the kaon and the pion are described in sect. 3. In sect. 4, the calculated spectra are compared with the available data on ^{12}C and ^{16}O. Conclusions follow in sect. 5, together with further discussions and comments concerning the question of consistency with Σ^- atom data, and of the difficulty in extracting information about the Σ-nucleus spin-orbit interaction.

2. Description of the model

2.1. RESPONSE FUNCTION FOR (K^-, π^+) REACTIONS

We use a DWIA framework to describe Σ-formation processes in the (K^-, π^+) reaction, as illustrated in fig. 1. The pion inclusive cross section for the in-flight reaction is given by

$$\frac{d^2\sigma}{d\Omega\, dE_\pi} = \frac{k_\pi E_\pi}{(2\pi)^2 v_K} \sum_f |\langle f, \pi|\hat{T}|i, K\rangle|^2 \delta(\omega - E_f + E_i)\,, \tag{1}$$

where $\omega = E_K - E_\pi$ is the energy transfer, k_π is the pion momentum, and $E_\pi = \sqrt{k_\pi^2 + m_\pi^2}$ is its energy; v_K is the velocity of the incident kaon with energy $E_K = \sqrt{k_K^2 + m_K^2}$, and $\hat{T}$ stands for the transition operator of the process. The state $|i\rangle$ refers to the initial ground state of the target nucleus, and $|f\rangle$ is a final Σ^- hypernuclear state. We are considering inclusive spectra, so that $\{|f\rangle\}$ represents the complete set of hypernuclear excited states, with $\Sigma|f\rangle\langle f| = 1$. In the distorted wave impulse approximation [17],

$$\langle f, \pi|\hat{T}|i, K\rangle = t_{KN\to\pi\Sigma}\langle f|\hat{O}|i\rangle\,, \tag{2}$$

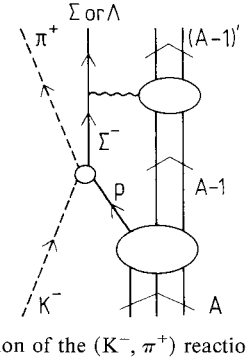

Fig. 1. Diagramatic representation of the (K^-, π^+) reaction within the DWIA framework.

where $t_{\mathrm{KN}\to\pi\Sigma}$ is the t-matrix for the elementary $\bar{\mathrm{K}}\mathrm{N}\to\pi\Sigma$ reaction and $\hat{O}$ is simply given by the overlap of the incoming kaon and outgoing pion waves:

$$\hat{O}=\sum_{j=1}^{A}\chi_{\pi}^{(-)*}(\boldsymbol{r}_j)\chi_{\mathrm{K}}^{(+)}(\boldsymbol{r}_j)\,. \tag{3}$$

(Here we have suppressed a trivial strangeness converting operator.) The distorted pion and kaon waves χ_π and χ_K are normalized in such a way that their product reduces to $\mathrm{e}^{i(\boldsymbol{k}_\mathrm{K}-\boldsymbol{k}_\pi)\cdot\boldsymbol{r}}$ in the free case, apart from the Coulomb distortion. The cross section (1) is then written as:

$$\frac{\mathrm{d}^2\sigma}{\mathrm{d}\Omega\,\mathrm{d}E_\pi}=\sigma_0 R(\omega)\,,$$

$$R(\omega)=\sum_{\mathrm{f}}|\langle\mathrm{f}|\hat{O}|\mathrm{i}\rangle|^2\delta(\omega-E_\mathrm{f}+E_\mathrm{i})\,, \tag{4b}$$

where σ_0 is a cross section of the elementary process,

$$\sigma_0=\frac{k_\pi E_\pi}{(2\pi)^2 v_\mathrm{K}}\left|t_{\mathrm{KN}\to\pi\Sigma}\right|^2. \tag{5}$$

The t-matrix $t_{\mathrm{KN}\to\pi\Sigma}$ is approximated by the free one, averaged over the momentum distribution of the nucleons. The structure of the Σ-formation spectra is then entirely determined by the response function $R(\omega)$. In the case of the stopped kaon experiment we calculate the partial width for population of a given hypernuclear state and sum over all these states. With the same approximations as discussed previously for the in-flight reaction we obtain for the stopped (K^-,π^+) rate from a K^- atomic orbit (nl):

$$\Gamma_{nl}(\mathrm{K}^-+{}^A Z\to\pi^++\mathrm{all})$$

$$=\frac{k_\pi E_\pi}{\pi}\left|t_{\mathrm{K}^-\mathrm{N}\to\pi^+\Sigma}\right|^2\frac{1}{2l+1}\sum_m\sum_{\mathrm{f}}\int\mathrm{d}\Omega_{\boldsymbol{k}_\pi}|\langle\mathrm{f}|\hat{S}_{nlm}|\mathrm{i}\rangle|^2\delta(\omega-E_\mathrm{f}+E_\mathrm{i})\,, \tag{6}$$

with

$$\hat{S}_{nlm}=\sum_{j=1}^{A}\chi_{\pi}^{(-)*}(\boldsymbol{k}_\pi,\boldsymbol{r}_j)\phi_{nl}(r_j)\,Y_{lm}(\hat{\boldsymbol{r}}_j)\,, \tag{7}$$

where we have again omitted a trivial strangeness conversion factor. Here ϕ_{nl} is the radial wave function of the bound state from which the kaon is absorbed. In our particular case, we assume that the kaon is in the 3d orbit [17]).

We will now continue with a discussion of the Σ single-particle states, which are of primary interest in the study of Σ hypernuclei.

2.2. COUPLED CHANNELS APPROACH

In a nuclear medium the Σ decays into a Λ via the $\Sigma\mathrm{N}\to\Lambda\mathrm{N}$ conversion process. The effects of such inelastic channels are commonly included in the imaginary part

of the Σ nuclear optical potential. We use here a more direct approach, namely to solve a $\Sigma \leftrightarrow \Lambda$ coupled channels problem which we now specify.

The basic coupled channels to be considered are the following:

(i) the $\Sigma+(A-1)$ system, in which the Σ hyperon moves in the environment of $A-1$ nucleons. The Σ experiences an average potential $V_\Sigma(r)$ which we assume to be a real Woods-Saxon potential. We assign a wave function $\psi_\Sigma(\boldsymbol{r})$ to this channel;

(ii) the $\Lambda+(A-1)'$ system, in which a Λ hyperon, generated by the $\Sigma^-\mathrm{p}\to\Lambda\mathrm{n}$ reaction, moves in the environment of $A-1$ nucleons which can be in a highly excited state: a large fraction of the $\Sigma-\Lambda$ mass difference $M_\Sigma - M_\Lambda \simeq 80$ MeV can go into nuclear excitations. We describe the $\Lambda+(A-1)'$ system as an effective two-body channel with a wave function $\psi_\Lambda(\boldsymbol{r})$ and an effective potential $V_\Lambda(r)$. Such an effective two-channel treatment of inelastic processes is familiar from a similar description of the global features of proton-antiproton annihilation channels, see ref. [18]).

The $\Sigma+(A-1)$ and $\Lambda+(A-1)'$ channels are assumed to be coupled by non-diagonal interactions $V_{\Sigma\Lambda} = V_{\Lambda\Sigma}$. In practice the strength of these interactions will be constrained by the observed widths of Σ^- atomic states.

The coupled channel equation is

$$[\nabla^2 + K^2(r)]\Psi(\boldsymbol{r}) = 0\,, \tag{8a}$$

with

$$\Psi = \begin{pmatrix} \Psi_\Sigma \\ \Psi_\Lambda \end{pmatrix}, \tag{8b}$$

and

$$K^2 = 2\begin{pmatrix} M_\Sigma(\varepsilon_\Sigma - V_\Sigma) & M_\Sigma V_{\Sigma\Lambda} \\ \tilde{M}_\Lambda V_{\Lambda\Sigma} & \tilde{M}_\Lambda(\varepsilon_\Lambda - V_\Lambda) \end{pmatrix}, \tag{8c}$$

where ε_Σ and ε_Λ are the single-particle energies of the Σ and Λ hyperon, respectively. The total energy of the $\Sigma+(A-1)$ system is then:

$$E = M_\Sigma + \varepsilon_\Sigma + E_{A-1} = M_\Lambda + \varepsilon_\Lambda + E'_{A-1}\,.$$

For the potentials $V_\Sigma(r)$ and $V_\Lambda(r)$ we use Woods-Saxon forms:

$$V_{\Sigma,\Lambda}(r) = \frac{V^{(0)}_{\Sigma,\Lambda}}{1+\exp\left((r-R_0)/a\right)}, \tag{9}$$

with $R_0 = 1.1(A-1)^{1/3}$ fm and $a = 0.6$ fm. To V_Σ we also add the attractive Coulomb potential experienced by the Σ^- in the field of the residual nucleus. The parameters $V^{(0)}_\Sigma$ and $V^{(0)}_\Lambda$ will be specified later. An analogous parametrization is used for the coupling potentials $V_{\Sigma\Lambda}$ and $V_{\Lambda\Sigma}$, with corresponding strengths $V^{(0)}_{\Sigma\Lambda} = V^{(0)}_{\Lambda\Sigma}$. Note that since ψ_Λ represents effectively the full complexity of the $\Lambda+(A-1)'$ system, the mass parameter $\tilde{M}_\Lambda$ is not the free Λ mass, but includes the average energy transferred to the residual $A-1$ nucleons. From kinematical considerations we expect that $\tilde{M}_\Lambda$ should in fact be close to M_Σ, the Σ mass.

Given the Σ hyperon wave function ψ_Σ as obtained from the coupled channels scheme (8), the response function (4b) and the stopped kaon rate (6) are readily evaluated. The nuclear ground state $|\mathrm{i}\rangle$ is described by density-dependent Hartree-Fock wave functions [19]). Then the amplitudes $\langle \mathrm{f}|\hat{O}|\mathrm{i}\rangle$ and $\langle \mathrm{f}|\hat{S}|\mathrm{i}\rangle$ reduced to effective one-body matrix elements for the $\mathrm{N}\to\Sigma$ transition. Further details will be given in sect. 4.

3. Distorted waves of the K^- and π^+

Distorted wave functions for the incoming K^- and outgoing π^+ are generated from a non-local meson-nucleus optical potential. For the pion, medium effects such as nucleon Fermi motion, nucleon binding and Pauli blocking are incorporated by the method of refs. [20,21]), in which the pion, struck nucleon and spectator residual nucleus degrees of freedom are taken into account in the evaluation of the first-order optical potential. For the kaon, the following form of the momentum space optical potential is used:

$$U_{\mathrm{K}}(E;\boldsymbol{k},\boldsymbol{k}') = [b_0(E) + b_1(E)\hat{\boldsymbol{k}}\cdot\hat{\boldsymbol{k}}']\left(\frac{\alpha^2+k_0^2}{\alpha^2+k^2}\right)\left(\frac{\alpha^2+k_0^2}{\alpha^2+k'^2}\right)\rho(\boldsymbol{k}-\boldsymbol{k}')\,, \qquad (11)$$

with

$$b_i(E) = \frac{4\pi}{2E}\,\frac{P_{\mathrm{lab}}}{k_{\mathrm{c.m.}}}\,f_i(k_{\mathrm{c.m.}})\,.$$

Here k_0 is the on-shell momentum corresponding to the K-nucleus center-of-mass energy E, $\rho(\boldsymbol{k})$ is the momentum distribution of the target nucleus, and the amplitudes f_i are determined from the phase shift analysis [22]) of the elementary K^--nucleon scattering process. The amplitudes f_0 and f_1 correspond respectively to the $l=0$ and $l=1$ partial wave amplitudes. The $l=2$ and higher amplitudes are included in f_0.

In order to assess the above kaon optical potential, we calculate K^- elastic scattering on ^{12}C. Results of the differential cross sections for two choices of the non-locality range parameter: $\alpha = 300$ MeV and $\alpha = 600$ MeV/c are compared, in fig. 2, with the data [23]) at $P_{\mathrm{lab}} = 800$ MeV/c. The K^--nucleus interaction is dominated by absorptive processes, and thus the angular distributions are similar to those obtained by scattering from a black disk. The K^- distorted waves embody these attenuation effects.

The pion, on the other hand, does not interact so strongly with the target nucleus, since the pion energies of our interest here are not close to the $\Delta(1232)$ resonance. The pion distorted waves have been tested in calculations of pion elastic scattering and charge-exchange reactions on various nuclei in the energy region 50 MeV $< T_\pi <$ 500 MeV. The agreement with the data is good [21]).

Variations in the non-locality range α from 300 to 600 MeV/c for the K^- and π^+ change the forward cross section by only about 5%.

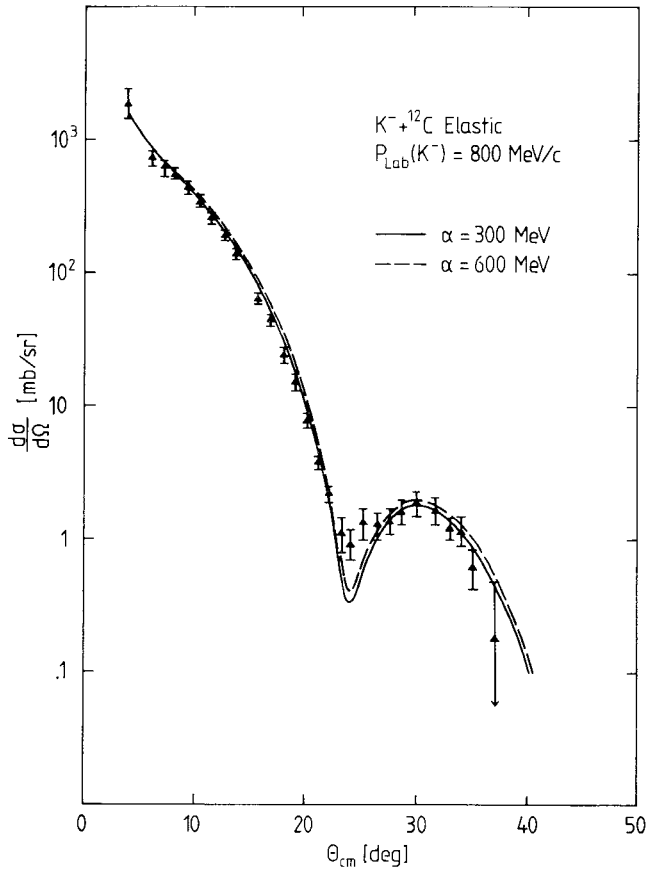

Fig. 2. Differential cross sections for the elastic scattering of K^- on ^{12}C, calculated with the optical potential (11) and two different non-locality range parameters α. The data are from ref. [23]).

In the stopped K^- experiment, the K^- capture dominantly from an atomic 3d-state [14]). Hence we assume that the initial K^- state is described by a single atomic 3d wave function solved numerically with a real K^- optical potential.

From the comparison between calculations with distorted waves and with plane waves, we find that the distortion effects do not bring about qualitative changes in the shape of the spectra, but reduce the cross section generally by a factor of about 4.

In the kaon-in-flight spectrum, a larger Σ excitation energy corresponds to a larger momentum transfer. On the other hand, in the stopped kaon experiment, a larger excitation energy means a smaller pion kinetic energy and thus a smaller momentum transfer. This momentum dependence of the transition operator $\hat{O}(\boldsymbol{r})$ has non-negligible effects on the calculated spectrum. The strengths at higher excitation energies are relatively enhanced in the kaon-in-flight spectrum and reduced in the stopped kaon one.

4. Results and discussion

Our calculated results are compared with data of the kaon-in-flight experiment on ^{12}C and ^{16}O (taken at CERN), and of the stopped kaon experiment on ^{12}C (taken at KEK). We present the results in two steps, with and without including the inelastic Σ-Λ coupled channel effects.

The experimental (K^-, π^+) spectra are given only in terms of counting rates, not in terms of normalized cross sections (or Σ-formation widths in the stopped kaon case). The calculated spectra therefore include an arbitrary normalization to match the overall magnitude of the data.

The location of the Σ threshold is determined essentially by the energy of the proton hole state. The hypernuclear excitation energy is

$$M_{\mathrm{HY}} - M_A = E_{\mathrm{K}} - E_\pi - T_{\mathrm{recoil}}\,, \tag{12}$$

where T_{recoil} is the recoil energy of the hypernucleus, assuimg a target nucleus at rest. Alternatively,

$$M_{\mathrm{HY}} - M_A = M_\Sigma - M_{\mathrm{p}} + \varepsilon_\Sigma - \varepsilon_{\mathrm{P}}\,, \tag{13}$$

in terms of the Σ mass M_Σ and single-particle energy ε_Σ, and of the proton mass M_{p} and single-particle energy ε_{p} (see table 1). The threshold value of eq. (13) is obtained with $\varepsilon_\Sigma = 0$; using for ε_{p} the energy of the uppermost occupied proton shell one finds

$$(M_{\mathrm{HY}} - M_A)_{\mathrm{threshold}} \simeq \begin{cases} 271.5 \text{ MeV for } ^{16}\mathrm{O} \\ 275 \text{ MeV for } ^{12}\mathrm{C}\,. \end{cases}$$

It is useful to introduce the Σ binding energy

$$B_\Sigma = (M_{\mathrm{HY}} - M_A)_{\mathrm{threshold}} - (M_{\mathrm{HY}} - M_A)\,. \tag{14}$$

The form of the Σ-nucleus single-particle potential has already been specified in sect. 2.2. We omit here a possible Σ-nucleus spin-orbit interaction for the moment, but commment on its role later in the discussion.

TABLE 1

Proton single-particle energies in MeV [ref. [27])]

Proton state	^{12}C	^{16}O
$p_{1/2}$		−12.5
$p_{3/2}$	−16	−19
$s_{1/2}$	−36	−44

4.1. RESPONSE FUNCTIONS WITHOUT Σ-Λ CONVERSION

Here we first present a series of results in which the Σ-Λ channel coupling is ignored by setting $V_{\Sigma\Lambda}$ and $V_{\Lambda\Sigma}$ equal to zero in eq. (8). The effect of the inelastic Σ-Λ conversion will be discussed separately in sect. 4.2.

4.1.1. Spectra derived from kaon-in-flight experiments. The ^{16}O spectrum measured at CERN [2]) has previously been interpreted as showing the existence of two narrow peaks at $B_\Sigma \simeq -7$ MeV and -13 MeV. Natural assignments in a shell model picture with quasibound states have been discussed in ref. [24]) in terms of $(p^{\Sigma}_{1/2}, p^{-1}_{1/2})$ and $(p^{\Sigma}_{3/2}, p^{-1}_{3/2})$ Σ-particle-proton-hole states, respectively. However, the present calculation with its presumably more realistic treatment of the particle-hole continuum does not verify a narrow peak at an energy as high as 13 MeV.

The fact that not much excitation strength has been observed in the energy region well below the Σ threshold can be used to restrict the strength of the Σ-nucleus single-particle potential V_Σ of eq. (9). A typical result for the ^{16}O spectrum is shown in fig. 3. Here the depth of the Σ potential is $V_\Sigma^{(0)} = -5$ MeV. The overall features of the (K^-, π^+) spectrum are evidently quite well reproduced, although the apparent narrow structures at excitation energies around 7 MeV and 13 MeV are not produced

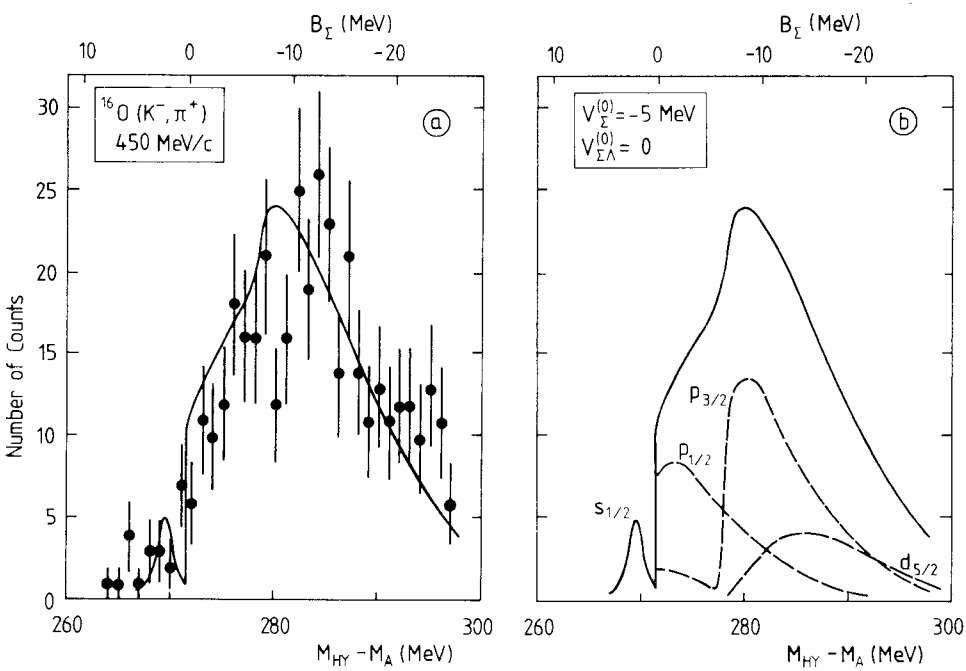

Fig. 3. Calculated ^{16}O(K^-, π^+) spectrum for the in-flight experiment at $p_K = 450$ MeV/c without Σ-Λ conversion effects. In part (a) the spectrum is compared with the experimental data [2]): In part (b) we show the contributions from different Σ^- states. The $s_{1/2}$ Σ-state shown explicitly is coupled to the $p_{1/2}$ nucleon hole state, other states are coupled to $p_{1/2}$ as well as $p_{3/2}$ nucleon hole states. Parameters used are shown in (b).

in this calculation. If the Σ potential strength is increased to $V_\Sigma^{(0)} = -10$ MeV, the lowest p-state would appear as a bound state just as the s-state, but this would lead to a spectrum which is qualitatively different from the experimental one. No significant changes appear when the Σ-Λ coupling potential $V_{\Sigma\Lambda}$ is turned on, as will be demonstrated in the next subsection.

The broad peak structure at $B_\Sigma \simeq -9$ MeV comes dominantly from the $(p^\Sigma_{3/2}, p^{-1}_{3/2})$ Σ-hole configuration. Since the proton $p_{3/2}$ state is more strongly bound (by about 6.5 MeV) than the proton $p_{1/2}$ state, the actual Σ single-particle energy corresponding to this maximum is $\varepsilon_\Sigma \simeq 2.5$ MeV. The peak at $B_\Sigma \simeq 2.5$ MeV is due to the transition from the proton in a $p_{1/2}$ state to the $s_{1/2}$ bound state of the Σ (the hypernuclear ground state in this model).

The measured in-flight (K^-, π^+) spectrum for ^{12}C is said to give indications of a narrow structure at $B_\Sigma \simeq -3$ MeV [ref. [2])]. A typical calculated result, using again $V_\Sigma^{(0)} = -5$ MeV as for ^{16}O, is presented in fig. 4. The overall agreement with the data is again good, although a narrow peak with a width as small as 5 MeV [ref. [2])] cannot be produced in this approach. As expected from the kinematical conditions of this experiment with its small momentum transfer $|q| \simeq 70$ MeV/c at threshold, the spectrum is dominated by the substitutional transition to a $(p^\Sigma_{3/2}, p^{-1}_{3/2})$ Σ-particle-proton-hole state.

The Σ-nucleus potential for ^{12}C has a smaller radius than the one for ^{16}O, so that within limits the depth $V_\Sigma^{(0)}$ can be increased without producing a bound p-state.

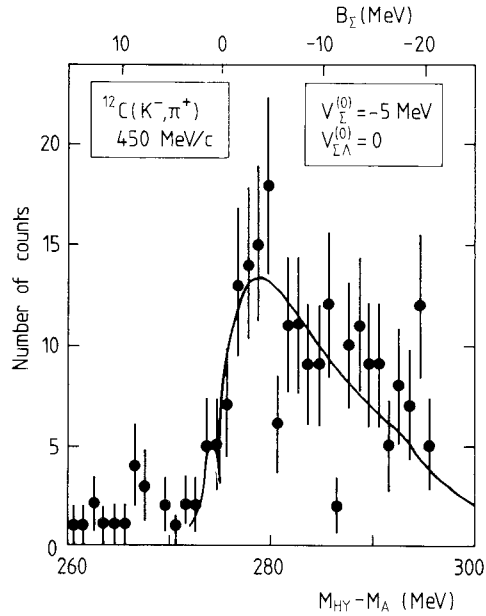

Fig. 4. Calculated $^{12}C(K^-, \pi^+)$ spectrum for the in-flight experiment at $p_K = 450$ MeV/c without Σ-Λ conversion effects using $V_\Sigma^{(0)} = -5$ MeV, compared with the experimental data [2]).

In order to examine the sensitivity of the spectrum with respect to changes of $V_\Sigma^{(0)}$, we show in fig. 5 results obtained with $V_\Sigma^{(0)} = -10$ MeV. The main effect of the increased Σ binding is evidently a narrowing of the $(p^{\Sigma}_{3/2}, p^{-1}_{3/2})$ particle-hole response function: the strength is now concentrated in the low energy region just above threshold. The overall agreement with data is still acceptable, given their large statistical errors.

4.1.2. Spectra derived from the stopped-kaon experiment. The striking feature of the π^+ spectrum for $^{12}C(K^-, \pi^+)$ with stopped kaon is the appearance of three narrow peaks reported in ref. [4]). Because of the large momentum transfer $|q| \simeq$ 170 MeV/c in this experiment, one expects that more than just substitutional Σ-particle-proton-hole states will be excited. In a quasibound state picture, one might tentatively associate two of the three peaks with $(p^{\Sigma}_{3/2}, p^{-1}_{3/2})$ and $(p^{\Sigma}_{1/2}, p^{-1}_{3/2})$ states [24]). However, the narrow structures in question are all located in the region of unbound Σ states, so that a careful treatment of the Σ continuum and of the Σ-Λ conversion effects is certainly required.

Following the same procedure as before, we have calculated the stopped kaon rate for $^{12}C(K^-, \pi^+)$ using Σ-potential depths $V_\Sigma^{(0)} = -5$ MeV and -10 MeV, respectively. The results without inclusion of the Σ-Λ channel coupling are shown in fig. 6. For the stronger potential with $V_\Sigma^{(0)} = -10$ MeV, some $(p^{\Sigma}_{3/2}, p^{-1}_{3/2})$ strength is

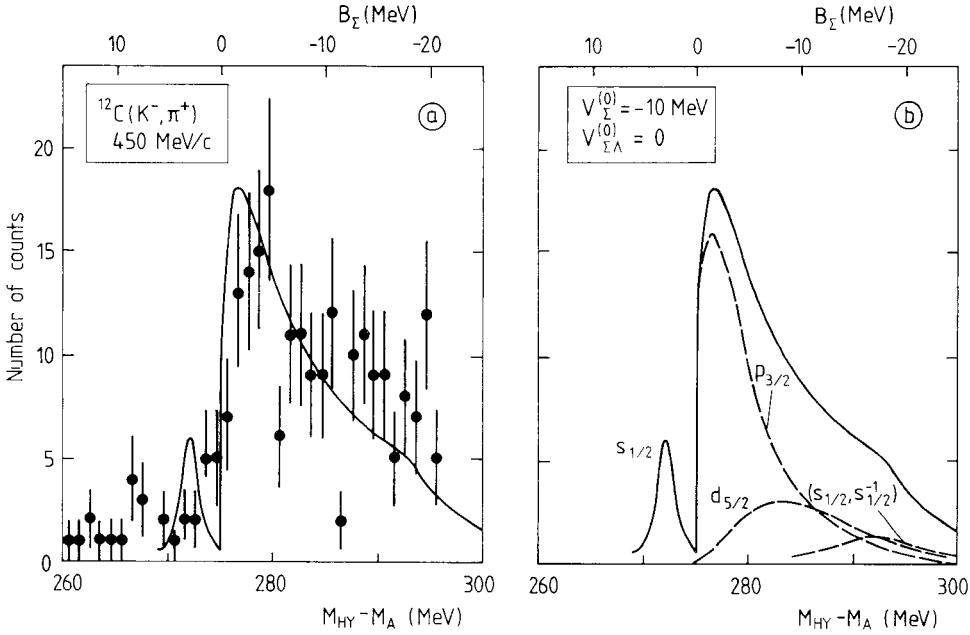

Fig. 5. Calculated $^{12}C(K^-, \pi^+)$ spectrum for the in-flight experiment at $p_K = 450$ MeV/c without Σ-Λ conversion effects. In part (a) the spectrum is compared with the experimental data [2]). Part (b) shows the contribution from different Σ^- states coupled to the $p_{3/2}$ nucleon hole state. Parameters used are given in (b).

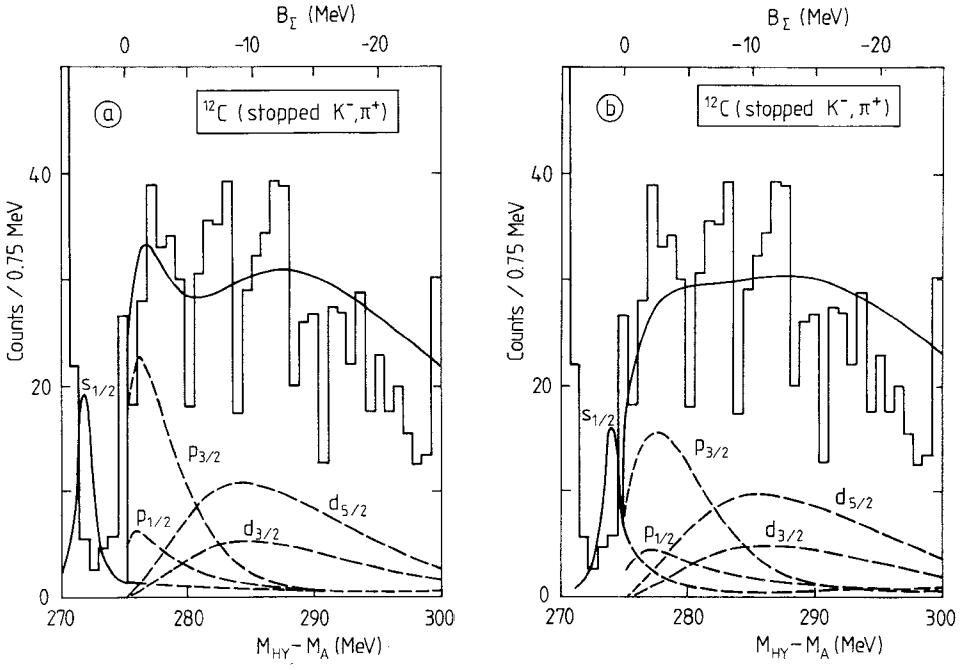

Fig. 6. Calculated $^{12}C(K^-, \pi^+)$ spectra for the reaction with stopped kaons, without Σ-Λ conversion effects. Part (a) shows the result for $V_\Sigma^{(0)} = -10$ MeV, part (b) for $V_\Sigma^{(0)} = -5$ MeV. The contributions from different Σ^- states coupled to the $p_{3/2}$ nucleon hole state are indicated.

concentrated at low energy such that a peak structure appears. However, one has to keep in mind that the Σ-Λ inelastic conversion effects broaden this structure, as we shall see. It is therefore difficult, if not impossible, to understand the appearance of narrow peaks in a conventional continuum calculation.

4.2. INCLUSION OF Σ-Λ CONVERSION EFFECTS

We investigate now the role of inelastic channels based on the $\Sigma N \to \Lambda N'$ process which is treated in the approximate coupled channels scheme of sect. 2.2. This requires a discussion of the Σ-Λ coupling potential $V_{\Sigma\Lambda}$ in eq. (8c).

Some constraints on $V_{\Sigma\Lambda}$ arise from the analysis of Σ^--atomic level shifts and widths due to strong interactions. For example, Batty *et al.* [25]) have systematically investigated the Σ^- atomic transitions. We concentrate here on the case of ^{28}Si which is the one with the smallest statistical errors [25]). It was found that the corresponding level shifts and widths could be reproduced with a complex Σ^- optical potential

$$V_\Sigma^{\mathrm{opt}}(r) = (U_\Sigma^{(0)} + iW_\Sigma^{(0)}) \frac{\rho(r)}{\rho_0}, \tag{15a}$$

with

$$\rho(r) = \frac{\rho_0}{1+\exp\left[(r-R_0)/a\right]}, \tag{15b}$$

using the parameters $U_\Sigma^{(0)} = -26$ MeV, $W_\Sigma^{(0)} = -14$ MeV, $R_0 = 2.98$ fm (for the example of ^{28}Si), $a = 0.55$ fm. The imaginary part $W_\Sigma^{(0)}$ should reflect, in particular, the Σ-Λ inelastic transition in the nuclear environment. This would then indicate a large width $\Gamma_\Sigma \sim -2W_\Sigma^{(0)} \simeq 30$ MeV, and consequently a large coupling potential $V_{\Sigma\Lambda}$. We note, however, that the results for the atomic width and shift are extremely sensitive to the choice of the radius parameter R_0. The value of R_0 used by Batty *et al.* [25]) is determined from electron scattering. However, the radius of the average potential experienced by the sigma is not necessarily the same as the radius of the nuclear charge density. We use a slightly larger value given by $R_0 = 1.1\, A^{1/3}$ fm, a standard choice for hypernuclear as well as nuclear shell model calculations. With this radius we found agreement with the measured shifts and widths for $V_\Sigma^{(0)} \simeq -10$ MeV together with a Σ-Λ coupling potential $V_{\Sigma\Lambda}$ of comparable magnitude. These are the values which we use for orientation. Similar conclusions have been reached by Batty, Gal and Toker in ref. [25]).

Let us now return to the calculation of the (K^-, π^+) spectra using the coupled channels scheme (8). We found that a best choice for the effective mass parameter $\tilde{M}_\Lambda$ in eq. (8c) is $\tilde{M}_\Lambda = 0.99 M_\Sigma$. This corresponds to a kinematical situation in which about 70 MeV out of the mass difference $M_\Sigma - M_\Lambda \simeq 80$ MeV are transferred into excitations of the residual nucleus. The potential V_Λ is set equal to zero. Its influence has been found to be only marginal.

The (K^-, π^+) response function for ^{16}O obtained by solving the coupled channels equations (8) are shown in fig. 7. The Σ mean field is kept at the value $V_\Sigma^{(0)} = -5$ MeV as in fig. 3. As expected, the spectrum now becomes broader due to the inelastic Σ-Λ couplings. However, the additional widths do not change the gross features of the spectrum: The overall agreement with data is still satisfactory. In this calculation the peak representing the transition to the bound s-state of the Σ has a full width of about 1 MeV.

Similar results are obtained for the kaon-in-flight spectrum for ^{12}C. Again the Σ response function becomes broader (see fig. 8) due to the Σ-Λ conversion effect, but there are no qualitative changes.

A typical coupled-channels result for the spectrum corresponding to the stopped kaon experiment on ^{12}C is shown in fig. 9. Again the primary effect of a non-zero $V_{\Sigma\Lambda}$ is the broadening of the spectrum due to the spreading of strength over several states.

Finally, we discuss the sensitivity of this result with respect to variations of the potential V_Σ. For example, in the absence of the channel coupling potential $V_{\Sigma\Lambda}$, it was found that a Σ-potential with $V_\Sigma^{(0)} = -10$ MeV is sufficiently strong to produce a relatively narrow peak close to threshold (see fig. 6a). However, when the Σ-Λ

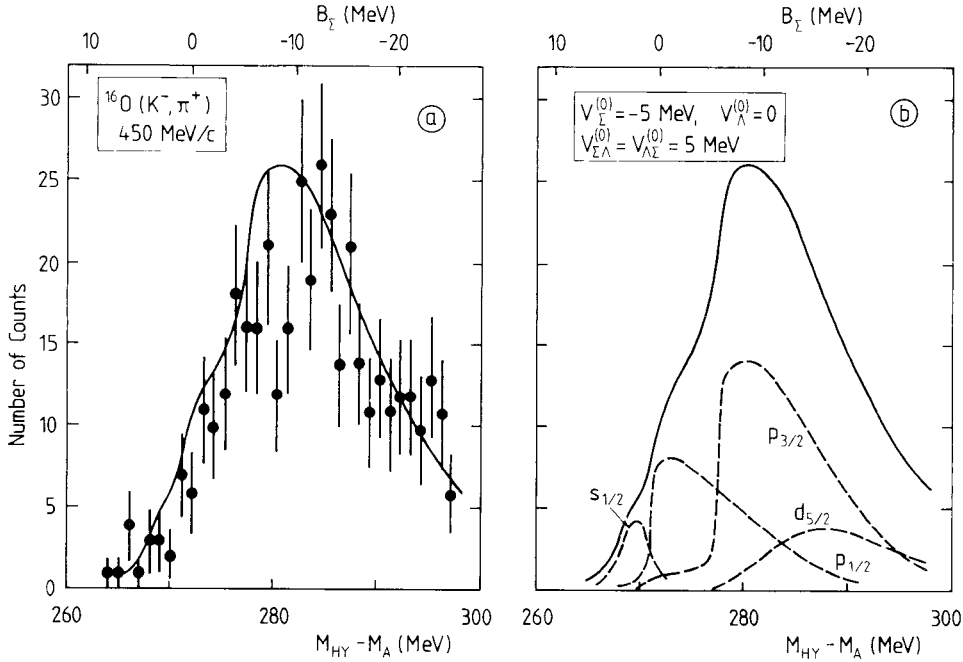

Fig. 7. Same as fig. 3, but with inclusion of Σ-Λ conversion effect.

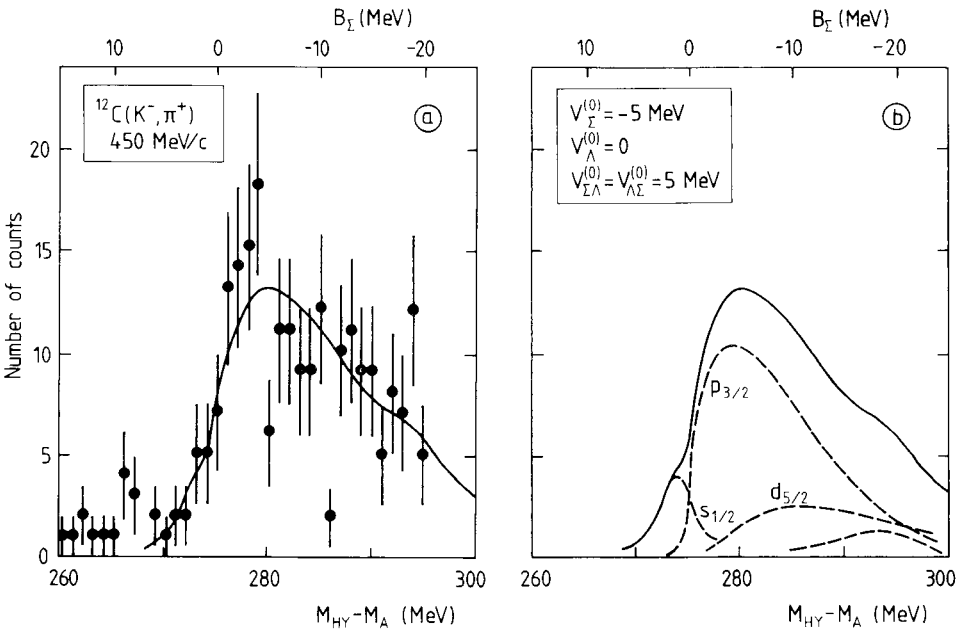

Fig. 8. Same as fig. 5, but with inclusion of Σ-Λ conversion effect.

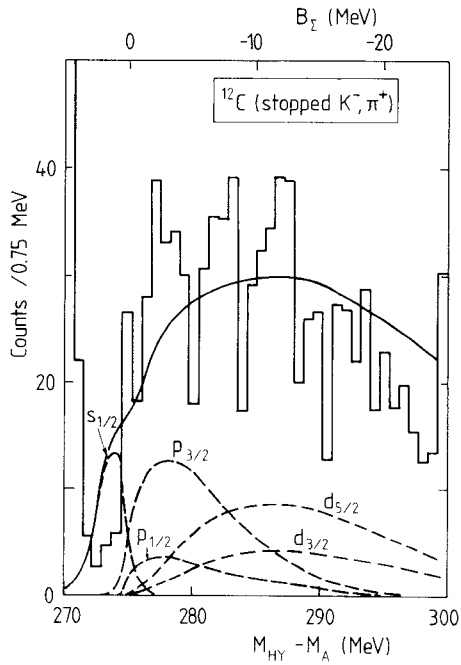

Fig. 9. Same as fig. 6b, but with inclusion of the Σ-Λ conversion effect.

coupling is turned on, the spreading of the excitation strength causes this peak structure to disappear, and one obtains a response function which is qualitatively similar to the one of fig. 6b. Thus, in the present framework, we see no straightforward way to generate narrow peaks in any of the spectra which have so far been studied experimentally.

5. Summary and conclusions

We have performed systematic response function calculations of Σ hyperon formation spectra as seen in (K^-, π^+) reactions. The primary aim of this investigation has been to provide an appropriate treatment of the unbound Σ states and to explore the influence of inelasticities related to the $\Sigma N \to \Lambda N'$ conversion process in nuclei. This is an extension of previous work [24]) in which Σ-hypernuclear spectra have been described in terms of quasibound states. The main conclusions of the present approach are summarized as follows:

5.1. STRENGTH OF THE Σ-NUCLEUS CENTRAL POTENTIAL

The gross features of Σ formation spectra from $^{12}C(K^-, \pi^+)$ and $^{16}O(K^-, \pi^+)$ are reproduced assuming a weakly attractive Σ-nucleus potential with a strength $V_\Sigma^{(0)}$ between -5 MeV and -10 MeV. However, such a potential does not support narrow quasibound states. In particular, the appearance of three narrow structures reported

in the $^{12}C(K^-, \pi^+)$ experiment with stopped kaons does not find a natural explanation within the present framework. It is possible to produce one narrow state close to threshold by increasing the depth of the Σ potential. However, this structure tends to be smeared out by the inelastic Σ-Λ conversion effects which redistribute the strength over a wider energy region.

5.2. COMPARISON WITH STRONG INTERACTION EFFECTS IN Σ^- ATOMS

We have re-investigated the strong interaction shifts and widths of Σ atomic orbits in order to examine their overall consistency with the Σ hypernuclear spectra. It was found that the empirical shifts and widths can be understood with a Σ central potential $V_\Sigma^{(0)} = -10$ MeV and a strength $|V_{\Sigma\Lambda}^{(0)}| \simeq 10$ MeV of the $\Sigma N \leftrightarrow \Lambda N$ coupling potential, using $R_0 = 1.1\, A^{1/3}$ fm as the radius parameter of the corresponding Woods-Saxon potential forms. The bulk structure of the Σ hypernuclear spectra suggests a smaller magnitude of $V_{\Sigma\Lambda}$ (typically about one half of the $V_{\Sigma\Lambda}^{(0)}$ derived from the width of Σ atomic states). We do not believe that the accuracy of presently existing data permits drawing further conclusions about the significance of this difference.

5.3. NOTE ON THE Σ-NUCLEUS SPIN-ORBIT INTERACTION

We have systematically investigated the sensitivity of the Σ-hypernuclear continuum spectra with respect to the Σ-nucleus spin-orbit potential. The strength of this potential has been varied between zero and values comparable to the nucleon-nucleus spin-oribt force. We found that such a variation, if accompanied by an appropriate change of the Σ-nucleus central potential, does not alter the overall shape of the spectra significantly. In particular, a narrow $p_{1/2}$ peak does not appear visibly in the (K^-, π^+) spectrum with stopped kaons. The main effect of the Σ spin-orbit interaction is a moderate rearrangement of the relevant partial wave contributions to the (K^-, π^+) response function. A quantitative discussion of the Σ nuclear spin-orbit coupling is therefore not (yet) within reach [see also ref. [26])].

The common feature of this and other related analysis is the observation that the Σ-nuclear interaction is weak, certainly much weaker than the interaction experienced by a nucleon in the nucleus. At the same time, there is an obvious need for data with higher statistics to draw more quantitative conclusions. In particular, should the existence of narrow Σ hypernuclear states be confirmed, then this would imply the presence of mechanisms which lead beyond our continuum response function framework.

References

1) R. Bertini *et al.*, Phys. Lett. **90B** (1980) 375
2) R. Bertini *et al.*, Phys. Lett. **136B** (1984) 29;
R. Bertini *et al.*, Phys. Lett. **158B** (1985) 19

3) H. Piekarz *et al.*, Phys. Lett. **110B** (1982) 428
4) T. Yamazaki *et al.*, Phys. Rev. Lett. **54** (1985) 102;
T. Yamazaki *et al.*, Nucl. Phys. **A450** (1986) 10
5) A. Gal and C.B. Dover, Phys. Rev. Lett. **44** (1980) 379 and 962 (E);
J. Dabrowski and J. Rozynek, Phys. Rev. **C23** (1981) 1706;
R. Brockmann and E. Oset, Phys. Lett. **118B** (1982) 33;
Y. Yamamoto and H. Bando, Prog. Theor. Phys. **69** (1983) 1312
6) J. Johnstone and A.W. Thomas, Nucl. Phys. **A392** (1983) 409
7) Y. Yamamoto and H. Bando, Prog. Theor. Phys. Suppl. **81** (1985) 9
8) M.M. Nagels, T.A. Rijken and J.J. de Swart, Phys. Rev. **D15** (1977) 2547
9) A. Gal, G. Toker and G. Alexander, Ann. of Phys. **137** (1981) 341
10) O. Morimatsu and K. Yazaki, Nucl. Phys. **A435** (1985) 727;
O. Morimatsu, Ph.D. thesis (Univ. of Tokyo, 1986), unpublished;
O. Morimatsu and K. Yazaki, Contr. paper to the 1986 INS-Sump. on Hypernuclear physics (1986) p. 1
11) H. Feshbach, Phys. Lett. **168B** (1986) 318
12) H.J. Pirner, Phys. Lett. **85B** (1979) 190;
O. Morimatsu *et al.*, Nucl. Phys. **A420** (1984) 573;
Y. He, F. Wang and C.W. Wong, Nucl. Phys. **A451** (1986) 653
13) R. Brockmann, Phys. Lett. **104B** (1981) 256;
A. Bouyssy, Nucl. Phys. **A381** (1982) 445;
C.B. Dover and A. Gal, Progr. Part. Nucl. Phys. **12** (1984) 171
14) T. Kishimoto, Nucl Phys. **A450** (1986) 447c
15) R.E. Chrien, E.V. Hungerford and T. Kishimoto, BNL-preprint 1986
16) J. Zofka, Invited talk at the 1986 INS-Symp. on Hypernuclear physics, Tokyo;
R. Wünsch and J. Zofka, Contr. paper to the 1986 INS-Sump. on Hypernuclear physics (1986) 17
17) J. Hüfner, S.Y. Lee and H.A. Weidenmüller, Nucl. Phys. **A234** (1974) 429
18) P.H. Timmers, W.A. van der Sanden and J.J. de Swart, Phys. Rev. **D29** (1984) 1928
19) X. Campi and D.W.L. Sprung, Nucl. Phys. **A194** (1972) 401;
M. Kohno, Nucl. Phys. **A410** (1983) 349
20) H. Garcilazo and W.R. Gibbs, Nucl. Phys. **A356** (1981) 284
21) W.B. Kaufmann and W.R. Gibbs, Phys. Rev. **C28** (1983) 1286;
also see W.R. Gibbs, W.B. Kaufmann and P.B. Siegel, The ABC's of pion charge exchange, in Proc. of the LAMPF Workshop on Pion double charge exchange, LA-10550-c, Los Alamos NATIONAL Laboratory, 1985
22) G.P. Gopal *et al.*, Nucl. Phys. **B119** (1977) 362
23) D. Marlow *et al.*, Phys. Rev. **C25** (1982) 2619
24) R. Hausmann and W. Weise, Z. Phys. **A324** (1986) 355;
see also J. Zofka, Nucl. Phys. **A450** (1986) 165c
25) C.J. Batty *et al.*, Phys. Lett. **74B** (1978) 27;
C.J. Batty, A. Gal and G. Toker, Nucl. Phys. **A402** (1983) 349
26) C.B. Dover et al., Phys. Rev. Lett. **56** (1986) 119
27) P. Kitching, W.J. McDonald, Th.A.J. Maris and C.A.Z. Vasconcellos, Adv. Nucl. Phys. **15** (1985) 43, and refs. therein